J. Astrophys. Astr. (2021) 42:79
https://doi.org/10.1007/s12036-021-09758-8

Can a regular black hole be observationally distinguished from singular black holes as spinning lens partner in PSR-BH binaries?

G. Y. TULEGANOVA[1], R. K. H. KARIMOV[1], R. N. IZMAILOV[1,2,*] and K. K. NANDI[1,3]

[1]Zel'dovich International Center for Astrophysics, M. Akmullah Bashkir State Pedagogical University, 3A, October Revolution Street, Ufa 450008, RB, Russia.
[2]Institute of Molecule and Crystal Physics, Ufa Federal Research Centre, Russian Academy of Sciences, 10 Prospekt Oktyabrya 151, Ufa 450075, Russia.
[3]High Energy Cosmic Ray Research Center, University of North Bengal, Darjeeling 734 013, India.
Corresponding Author. E-mail: izmailov.ramil@gmail.com

MS received 20 July 2020; accepted 6 March 2021

Abstract. To answer the question posed in the title, we consider a novel diagnostic, viz., the difference in the time of arrival (TOA) at the observer of two light rays that simultaneously emanate from a source behind a spinning lens and pass by either side of the lens to reach the observer. This is completely different from the usual Shapiro gravitational time delay, where only one onward light ray is reflected back to the observer. The TOA essentially samples the frame dragging caused by the spinning lens, apart from other lens parameters. Assuming a charged regular Ayón-Beato and García black hole as the spinning lens partner in some typical astrophysical pulsar black hole (PSR-BH) binaries, which provide the best laboratory for testing the TOA effect, we theoretically study how the prediction depends on the gyromagnetic ratio (Q/M) and how it compares with those when the role of spinning lens partner is played by the centrally singular Kerr–Newman and Kerr black holes. The numerical estimates for two illustrative binary lens systems show microsecond-level delay at the zeroth order, which should be measurable. However, the TOA predictions under thin-lens approximation are shown to differ only at third or higher orders of smallness indicating that the regular and singular black holes cannot be observationally distinguished despite significant qualitative differences existing among them.

Keywords. Spinning black hole—time of arrival.

1. Introduction

The Ayón-Beato and García black hole (AGBH) is a new class of static spherically symmetric regular exact solutions of general relativity (GR) coupled to nonlinear electrodynamics (Ayón-Beato & García 1998). See also Bronnikov (2000) for a very illuminating discussion of the solution. The aim of the study by Ayon-Beato & Garcia (1998) was to solve what the authors called one of the "mysterious" properties of a black hole—the central singularity—which is usually considered as one of the defects of GR. The AGBH solution of GR indeed removes the defect—the singularity disappears on account of the coupling of gravity to nonlinear electrodynamics. One may imagine that at each point in space–time the interaction of gravitation and nonlinear electromagnetism regularizes both fields. The solution corresponds to a regular BH when the gyromagnetic ratio $|Q|/M \leq 0.634$, where Q is the charge and M is the asymptotic ADM mass. The curvature invariants and the electric field are regular everywhere including at the origin.

Manko & Ruiz (2016) demonstrated that the total energy of an electromagnetic field in the static AGBH is equal to only the ADM mass parameter M independent of the charge parameter Q. This result supports the original idea of Born & Infeld (1934a,b) to use nonlinear electrodynamics for proving the electromagnetic nature of mass. Toshmatov (2015) studied scalar, electromagnetic, and gravitational test fields in the AGBH space–time and showed that the damping of the quasi-normal modes in regular black hole space–times is suppressed in comparison with the case of

Published online: 17 July 2021

Schwarzschild black holes. Further, increasing the charge parameter of the regular black holes increases the reflection and decreases the transmission factor of incident waves for each of the test fields. Nandi (2020) have shown that the famous hoop conjecture (due to Thorne) is not violated in the AGBH space–time. These are some of the interesting features of the static AGBH.

For our theoretical study, we shall need a spinning AGBH to act as a lens in typical astrophysical binary systems. Using the well-known Newman–Janis algorithm (Newman & Janis 1965), the static, spherically symmetric, and charged AGBH has been converted by Toshmatov (2014) into a spinning AGBH that shows a number of interesting properties: it is also regular and the critical value of the electric charge Q, for which two horizons merge into one, sufficiently decreases in the presence of nonvanishing spin a of the black hole (Toshmatov 2014). Abdujabbarov *et al.* (2016) showed that the radius of the shadow cast by the spinning AGBH decreases monotonically and the distortion parameter increases when the value of total mass M, rotation parameter a, and electric charge Q increase. Along the line of exploring other interesting features, we shall consider the time of arrival (TOA) effect under thin-lens approximation. Both the concepts are explained below.

The difference in the TOA at the observer is a potential new observable, first conceived by Dymnikova (1984, 1986) to our knowledge, that samples the frame-dragging effect caused by a spinning lens. Consider a binary system, where a variable light source S (pulsar) orbits a spinning compact lens (BH). As illustrated in Figure 1, suppose two light rays simultaneously emanate from the source S behind a spinning lens L (with mass M and spin a), pass on either side of the lens to reach the observer at O, say, the Earth. The rays will reach at different times at O due to frame dragging caused by the intervening spinning lens. The dragging causes the light path lengths on either side of the lens to differ, shorter on the co-rotating side and longer on the counter-rotating side (Figure 1). The TOA at the observer is subtracted to sample the frame-dragging effect (absent for a static lens) and so the difference in TOA is also named "relative time delay" by Laguna & Wolszczan (1997). We wish to emphasize that the difference in the TOA is not the usual Shapiro gravitational time delay (Shapiro 1964) that appears even for a static lens. In this case, a single light ray, sent onward by an observer, passes by an intervening lens of mass M and reflected back to the observer by a distant object in superior conjunction. The total elapsed time at the observer is obtained by adding two-way travel times ($M \neq 0$) and compared with a similar total elapsed time in the flat space (assuming $M = 0$). Shapiro found the former time lapse to be larger than the latter, hence the terminology gravitational time delay.[1] He found the excess value to be $\delta t^{\rm Sch}_{\rm Shapiro} \sim 245\ \mu$s with Sun as the gravitating lens, which agrees with observation with remarkable accuracy.

The TOA loosely resembles an astrophysical analog of the quantum Bohm–Aharonov effect. It has first been calculated to the zeroth order by Laguna & Wolszczan (1997) in the Kerr metric for some hypothetical binary systems.[2] A similar, though not exactly the same, type of effect was studied by Datta and Kapoor (1985), where light rays were assumed to

[1]There is also a new interesting effect called gravitational time advancement first proposed by Bhafra & Nandi (2010). Its astrophysical implications are being investigated (Ghosh & Bhadra 2015; Deng & Xie 2017; Ghosh *et al.* 2019).

[2]We think that the influential work of Laguna & Wolszczan (1997) needs some clarification. The starting point, following Dymnikova (1984, 1986), is their Equation (1):

$$t^{\pm}(r,d) = \sqrt{r^2-d^2} + 2M\ln\left(\frac{r+\sqrt{r^2-d^2}}{d}\right) + M\left(\frac{r-d}{r+d}\right)^{1/2} + \frac{(15\pi-8)M^2}{4d} \mp \frac{4aM}{d},$$

where d is the impact parameter.

The first four are Shapiro terms and the last one is the frame dragging term. The relative time delay of two signals, emitted at point r_e, traveling in opposite directions around the black hole and arriving at point r_0 is obtained by subtracting $t^{\pm}$ yielding Equation (2) of Laguna & Wolszczan (1997):

$$\Delta t_s = \frac{16aM}{d}.$$

While this is a correct equation to leading order, there is an interpretational issue here. It is implied that the Shapiro terms, which represent gravitational slowing down of light along radial motion, have subtracted out. In contradistinction, as stated by Dymnikova (1984), the time difference Δt_s arises purely due to the difference in optical paths between the rays, meaning that the paths are asymmetrical about the optical axis due to different impact parameters $d_- = d_+ + a$. Hence, it is unlikely that the Shapiro slow down along two different paths would completely subtract out, leaving behind just Equation (2). It is unclear if the magnitude of residual slow down would be negligible compared to Δt_s. A more appropriate leading order delay is our Δt_1 in Equation (39) that does not involve the slow down residual and is based on realistic finite distance configuration. Further, it yields Equation (2) under the conditions $d_{OL}, d_{LS} \to \infty$ and thin-lens approximation $(a/d_+) \ll 1$ (see Section 4 for details). However, the correction to Equation (2) brought about by Equation (39) is very minute because of the approximations adopted in this paper but the clarification could still be important, when those approximations are waived.

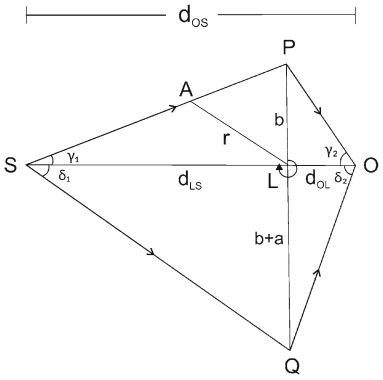

Figure 1. The generic thin-lens slender quadrilateral (here angles are exaggerated). *S*, *L*, and *O* are the source, lens, and observer, respectively, aligned on a straight line, *b* is the impact parameter and *a* is the spin with the axis perpendicular to the paper. The arbitrary angles (32)–(34) in Section 4 are as shown.

emerge not from a variable source behind the lens but from two diametrically opposite points on a spinning compact astrophysical object itself. A good example of TOA could be the early observation of extremely rapid fluctuations in the brightness of quasar 1525 + 227 with a characteristic time scale ~ 200 s speculated to be caused by a spinning black hole of mass $M \sim 5 \times 10^8 M_\odot$ situated between the quasar and the observer (Matilsky *et al.* 1982). Recently, TOA has been theoretically studied for the Johannsen metric (Izmailov 2019a) as a possible observable diagnostic to test the validity of the so-called "no-hair" conjecture of Penrose. The effect of the string parameter on TOA was investigated in Izmailov *et al*. (2020). So far no precise experimental data on TOA are available but very accurate future data from suitably identified binaries can constrain the values of the relevant deviation parameters. Such constraints were recently discussed also in the context of other modified gravity theories (Karimov 2018a,b; Kulbakova 2018; Tuleganova 2020; Tuleganova & Muhamadieva 2021).

We shall adopt thin-lens approximation (see details, in Hartle 2003), which applies to a situation where the source, lens, and observer are all considered as points and the light rays are assumed to travel in straight lines with the deflection taking place only at the lens and it works excellently when the rays travel vast distances compared to the lens size with the impact parameter far larger than the photon sphere. This means that the relevant angles making the quadrilateral in Figure 1 with the optical axis *SLO* are small. Thus, the TOA considered here is essentially a weak field effect due to the thin-lens approximation. A more accurate calculation of TOA should involve integration between two finite points *S* and *O* on the optical axis of the exact null geodesic around the spinning lens. Nonetheless, the thin-lens approximation provides a "simple and elegant description of many realistic lensing situations" (Hartle 2003).

The purpose of the present paper is to quantitatively evaluate the differences in the TOA in three space–times, one is the everywhere-regular spinning charged AGBH and the other two are the well-known centrally singular spinning charged Kerr–Newman black hole (KNBH) and its chargeless limit of Kerr black hole (KBH). We shall then compare the values obtained in these space–times to see if and how much they differ from each other. To do that, we shall derive the influence of the frame dragging as well as other parameters of the spinning lens using the thin-lens approximation. The analytic expression for TOA is applied to some potential PSR-BH binaries assuming that the relevant BH data are independently known.

The paper is organized as follows. In Section 2, we briefly introduce the spinning AGBH and in Section 3, we derive the generic formula for the difference in the TOA. In Section 4, we explicitly calculate the TOA components using the thin-lens approximation. Section 5 contains numerical values for two binary systems and Section 6 concludes the paper. We shall take $G = 1$ and $c = 1$ unless specifically restored.

2. Spinning AGBH

The dynamics of the theory we are using is governed by the gravitational action *S* with the source of nonlinear electrodynamics (Ayón-Beato & García 1998):

$$S = \int \sqrt{-g} d^4x \left[\frac{1}{16\pi} R - \frac{1}{4\pi} \mathcal{L}(F) \right], \tag{1}$$

where R is the Ricci scalar and $\mathcal{L}$ is a function of $F = \frac{1}{4} F_{\mu\nu} F^{\mu\nu}$, where $F^{\mu\nu}$ is the electromagnetic strength. Using the Legendre transformation

$$\mathcal{H} \equiv 2F\mathcal{L}_F - \mathcal{L}, \tag{2}$$

where $\mathcal{L}_F \equiv \partial\mathcal{L}/\partial F$ and $\mathcal{H} \equiv \mathcal{H}(P)$ with $P = \frac{1}{4} P_{\mu\nu} P^{\mu\nu} = F\mathcal{L}_F^2$. The solution crucially depends on the choice of $\mathcal{H}(P)$, which for the static AGBH is

$$\mathcal{H}(P) = P \frac{\left(1 - 3\sqrt{-2Q^2P}\right)}{\left(1 + \sqrt{-2Q^2P}\right)^3} - \frac{3}{2sQ^2} \left(\frac{\sqrt{-2Q^2P}}{1 + \sqrt{-2Q^2P}} \right)^{5/2}, \tag{3}$$

where $s \equiv |Q|/2M$ is half of the gyromagnetic parameter, its critical values $s = s_c$ define the transition between the regimes of BH horizon and no horizon, and the invariant P is negative. The correspondence with linear Maxwell theory is achieved in the weak field ($P \ll 1$) when the usual electromagnetic strength tensor is recovered:

$$F_{\mu\nu} \equiv \left(\frac{\partial \mathcal{H}}{\partial P}\right) P_{\mu\nu}. \tag{4}$$

The spherically symmetric, asymptotically flat, static AGBH metric obtained from the Einstein equations is given by Ayón-Beato & García (1998):

$$\mathrm{d}\tau^2 = -A(r)\mathrm{d}t^2 + \frac{1}{A(r)}\mathrm{d}r^2 + r^2(\mathrm{d}\theta^2 + \sin^2\theta \mathrm{d}\psi^2), \tag{5}$$

$$A(r) = 1 - \frac{2Mr^2}{(r^2+Q^2)^{3/2}} + \frac{Q^2r^2}{(r^2+Q^2)^2}, \tag{6}$$

with the associated asymptotically vanishing nonlinear electric field E given by

$$E = Qr^4\left[\frac{r^2-5Q^2}{(r^2+Q^2)^4} + \frac{15}{2}\frac{M}{(r^2+Q^2)^{7/2}}\right]. \tag{7}$$

Using the Janis–Newman algorithm (Newman & Janis 1965), the spinning AGBH obtained in Toshmatov (2014) in the Boyer–Lindquist coordinates (t, r, θ, ϕ) reads

$$\mathrm{d}\tau^2 = -g_{tt}\mathrm{d}t^2 - 2g_{t\varphi}\mathrm{d}t\mathrm{d}\phi + g_{rr}\mathrm{d}r^2 + g_{\theta\theta}\mathrm{d}\theta^2 + g_{\phi\phi}\mathrm{d}\phi^2, \tag{8}$$

where

$$g_{tt} = f(r,\theta), \tag{9}$$

$$g_{t\varphi} = a\sin^2\theta[f(r,\theta)-1], \tag{10}$$

$$g_{rr} = \frac{\Sigma}{\Delta_{\mathrm{AGBH}}}, \tag{11}$$

$$g_{\theta\theta} = \Sigma, \tag{12}$$

$$g_{\phi\phi} = \sin^2\theta\left[\Sigma - a^2(f(r,\theta)-2)\sin^2\theta\right]. \tag{13}$$

The metric function $f(r,\theta)$ is given by

$$f(r,\theta) = 1 - \frac{2Mr\sqrt{\Sigma}}{(\Sigma+Q^2)^{3/2}} + \frac{Q^2\Sigma}{(\Sigma+Q^2)^2}, \tag{14}$$

with

$$\Delta_{\mathrm{AGBH}} = \Sigma f(r,\theta) + a^2\sin^2\theta, \quad \Sigma = r^2 + a^2\cos^2\theta. \tag{15}$$

To calculate the difference in the TOA, we need to calculate the null trajectory for the spinning AGBH (8)–(15) on the equatorial plane, $\theta = \pi/2$, whence $\sin\theta = 1$, $\cos\theta = 0$ and the function $f(r,\theta)$ reduces to a simple form [actually $A(r)$, just incidentally]:

$$f(r) = 1 - \frac{2Mr^2}{(r^2+Q^2)^{3/2}} + \frac{Q^2r^2}{(r^2+Q^2)^2}. \tag{16}$$

The metrics (8)–(15) do not reduce to KNBH, except under the weak field expansion, where $M/r, Q/r \ll 1$ in the equatorial plane ($\theta = \pi/2$). However, it reduces exactly to KBH at $Q = 0$. So, we separately write out the exact KNBH metric for calculating the TOA:

$$g_{tt} = \frac{a^2\sin^2\theta - \Delta_{\mathrm{KNBH}}}{\Sigma}, \tag{17}$$

$$g_{t\varphi} = \frac{a\sin^2\theta[\Delta_{\mathrm{KNBH}} - (r^2+a^2)]}{\Sigma}, \tag{18}$$

$$g_{rr} = \frac{\Sigma}{\Delta_{\mathrm{KNBH}}}, \tag{19}$$

$$g_{\theta\theta} = \Sigma, \tag{20}$$

$$g_{\phi\phi} = \frac{\sin^2\theta}{\Sigma}[(r^2+a^2)^2 - \Delta_{\mathrm{KNBH}}a^2\sin^2\theta], \tag{21}$$

$$\Delta_{\mathrm{KNBH}} = r^2 - 2Mr + Q^2 + a^2. \tag{22}$$

3. Difference in TOA

To derive the equation for the difference in the TOA, consider a null trajectory $\mathrm{d}\tau^2 = 0$ on the equatorial plane ($\theta = \pi/2$) in the generic metric (8) so that the coordinate time required for light rays along an infinitesimal null world line is given by

$$\mathrm{d}t_\pm = \frac{\mathrm{d}\phi}{g_{tt}}[-g_{t\phi} \pm h(r,\phi)], \tag{23}$$

where

$$h(r,\phi) \equiv \sqrt{g_{t\phi}^2 - g_{tt}\left\{g_{rr}\left(\frac{\mathrm{d}r}{\mathrm{d}\phi}\right)^2 + g_{\phi\phi}^2\right\}}. \tag{24}$$

We assume the passage of coordinate time to be positive for both $\pm$ sides of the lens. Hence, we identify $\mathrm{d}\phi > 0$ for light rays passing the lens by the co-rotating side (+) and $\mathrm{d}\phi < 0$ for the counter-rotating side (−), so that $\mathrm{d}t_+$ and $\mathrm{d}t_-$ are both positive. The

net difference between the two null rays in the TOA at the observer is also positive and is given by

$$\mathrm{d}t = \mathrm{d}t_- - \mathrm{d}t_+ = \frac{|\mathrm{d}\phi|}{g_{tt}}[g_{t\phi} + h(r,\phi)] - \frac{|\mathrm{d}\phi|}{g_{tt}}[-g_{t\phi} + h(r,\phi)] = \left|\frac{2g_{t\phi}}{g_{tt}}\right||\mathrm{d}\phi|. \quad (25)$$

The delay $\mathrm{d}t$ is due to the frame-dragging effect characterized by $(2g_{t\phi}/g_{tt})$, which we are going to compute in this paper. When the lens is not spinning, $g_{t\phi} = 0$, the path lengths of the light ray on both sides of the lens would be equal and there would be no difference in TOA at the observer, $\mathrm{d}t = 0$. Only when the lens is spinning the path lengths will differ—longer for counter-rotating and shorter for co-rotating sides—giving rise to the TOA, $\mathrm{d}t > 0$. We assume that the source, spinning lens, and the observer are aligned, that is, they are situated on a straight line (see Figure 1).

The rays on the equatorial plane are required to pass through the weak field so that the thin-lens approximation is valid, that is, the distance of the closest approach $r \gg r_{\mathrm{ph}}^{\pm}$ on either side of the lens. This large r ensures that, for a given lens of mass M and spin a, the quantity $(M/r) \ll 1$. We shall apply the generic Equation (25) to AGBH by expanding $(2g_{t\phi}/g_{tt})$ such that, to first order in a and up to third Post-post-Newtonian (PPN) order in (M/r), we obtain

$$\mathrm{d}t^{\mathrm{AGBH}} = |\mathrm{d}\phi|\left(\frac{1}{c}\right) \times \left[\frac{4aM}{r}\left\{1 + \frac{2M}{r}\lambda_1 + \frac{M^2}{2r^2}\lambda_2 + \cdots\right\}\right], \quad (26)$$

where

$$\lambda_1 = 1 - \frac{Q^2}{4M^2}, \quad \lambda_2 = 8 - \frac{7Q^2}{M^2}. \quad (27)$$

For the KNBH, likewise, we obtain

$$\mathrm{d}t^{\mathrm{KNBH}} = |\mathrm{d}\phi|\left(\frac{1}{c}\right) \times \left[\frac{4aM}{r}\left\{1 + \frac{2M}{r}\xi_1 + \frac{M^2}{2r^2}\xi_2 + \cdots\right\}\right], \quad (28)$$

where the deviation parameters are

$$\xi_1 = 1 - \frac{Q^2}{4M^2}, \quad \xi_2 = 8 - \frac{4Q^2}{M^2}. \quad (29)$$

The KBH values ($Q = 0$) are retrieved when the deviation parameters assume values $\lambda_1 = \xi_1 = 1$ and $\lambda_2 = \xi_2 = 8$. Note that the factor $(4aM/r)$ multiplying the curly brackets in Equations (26) and (28) need not in general be small due to the presence of spin $a \sim M$. However, it will be seen that practical values associated with the binaries ensure that the terms $a(M/r)^2$ and $a(M/r)^3$ decay very rapidly making the series within the square brackets in (26) and (28) converge, leaving the leading order term $(4aM/r)$ to be the main contributor to $\mathrm{d}t$.

The total difference in the TOA Δt^{AGBH} between two null rays traveling from the source to the observer along two opposite sides of the intervening spinning lens is

$$\Delta t^{\mathrm{AGBH}} = \left(\frac{1}{c}\right)\int_0^{\pi}\mathrm{d}\phi \times \left[\frac{4aM}{r}\left\{1 + \frac{2M}{r}\lambda_1 + \frac{M^2}{2r^2}\lambda_2 + \cdots\right\}\right], \quad (30)$$

$$\equiv \frac{1}{c}(I_1 + I_2 + I_3) = \Delta t_1 + \Delta t_2 + \Delta t_3. \quad (31)$$

We shall compute the integral locating the spinning lens at the origin of a polar system of coordinates on the equatorial plane ($\theta = \pi/2$). As can be seen, (Q^2/M^2) does not influence the leading first-order term $\Delta t_1^{\mathrm{AGBH}}$. In the following, we shall derive explicit expressions for $\Delta t_1^{\mathrm{AGBH}}$, $\Delta t_2^{\mathrm{AGBH}}$, and $\Delta t_3^{\mathrm{AGBH}}$ within the thin-lens approximation.

4. Thin-lens approximation

In realistic lensing configurations, the radius over which bending takes place is of the order of Schwarzschild radius, which is much smaller than the typical distances d_{OL}, d_{OS}, and d_{LS} over which light propagates. Then, to an excellent approximation, light rays can be assumed to propagate as straight lines when far away from the lens, with the bending taking place only at the point lens (Hartle 2003). In a spinning lens situation, we argue that the approximation requires three additional nontrivial conditions to be satisfied as enumerated below.

(i) The first condition is that the rays emerging from S, after passing along line segments on either side of spinning lens L in the equatorial plane, should meet exactly at O making a quadrilateral $SPOQ$ of Figure 1. The angles are related by

$$\gamma_1 + \gamma_2 + \measuredangle OPS = \pi = \measuredangle OPS + \theta_1 \Rightarrow \gamma_1 + \gamma_2 = \theta_1, \quad (32)$$

$$\delta_1 + \delta_2 + \measuredangle OPS = \pi = \measuredangle OPS + \theta_2 \Rightarrow \delta_1 + \delta_2 = \theta_2. \quad (33)$$

In the thin-lens approximation, the relevant angles given below

$$\gamma_1 = \frac{b}{d_{LS}},\ \gamma_2 = \frac{b}{d_{OL}},\ \delta_1 = \frac{b+x}{d_{LS}},\ \delta_2 = \frac{b+x}{d_{OL}}, \tag{34}$$

should be small, where b is the impact parameter, $x(a, b)$ is an unknown function to be determined. For a given d_{OL}, the ratio $\chi\ (= d_{LS}/d_{OL})$ should be such that the angles $\gamma_1, \gamma_2, \delta_1, \delta_2 \ll 1$. Following the Boyer–Lindquist formula (Boyer & Lindquist 1967) for the bending of light at P and Q, respectively, we have

$$\theta_1 = \frac{4M}{b}\left(1 - \frac{a}{b}\right), \quad \text{(prograde motion of light)}, \tag{35}$$

$$\theta_2 = \frac{4M}{b}\left(1 + \frac{a}{b+x}\right), \quad \text{(retrograde motion of light)}. \tag{36}$$

Neglecting $(a/b)^2$ and higher orders, we get from the quadrilateral geometry, the root $x = a$, yielding two impact parameters b and $b + a$ on either side as shown in Figure 1.

(ii) The second condition is that the light rays should pass far away from the spinning lens that their trajectories can be approximated by straight lines. To determine how far is far, we need to know the radii of the photon spheres $r_{\rm ph}^{\pm}$ appearing, respectively, on the co-rotating (+) and counter-rotating sides (−) of the lens. For our purposes, we can safely take the Kerr value $r_{\rm ph}^{\pm} = 2M[1 + \cos\{\frac{2}{3}\arccos(\mp a/M)\}]$ giving an approximate idea of its location and assume the light ray to be traveling in the weak field region at an impact parameter far larger than the photon sphere.

(iii) Thin lens approximation breaks down when $\frac{M}{b} \sim O(1)$. Therefore, to avoid it, the third condition is that the smaller of the two impact parameters must far exceed the larger of the two radii $r_{\rm ph}^{\pm}$ of photon spheres, viz., $b \gg r_{\rm ph}^{-}$ or let $b = 10^n r_{\rm ph}^{-}$, where $n > 1$ is any real number. Our idea is to march b toward $r_{\rm ph}^{-}$ to the extent that the rays preserve the smallness of the angles in Figure 1 as discussed in (i). This algorithm will be exercised to produce Tables 1 and 2.

Returning to Figure 1, we have by construction $d_{LS} = \chi d_{OL}$, where $\chi > 0$ is a finite constant, $PLQ \perp OLS$, and the arbitrary angles are as indicated. The radial distance is measured from the lens L. By piecewise integration of the polar straight lines in the counter-rotating $(1/r_{\rm cou})$ and co-rotating $(1/r_{\rm cor})$ sectors, we straightforwardly derive the final result by subtracting the integrals over the path lengths, viz., $SQO - SPO$:

$$I_1 = 4aM\left[\int_{-\pi/2}^{-\pi} \frac{1}{r_{\rm cou}}\mathrm{d}\phi + \int_{0}^{-\pi/2} \frac{1}{r_{\rm cou}}\mathrm{d}\phi\right], \tag{37}$$

$$I_1 = -4aM\left[\int_{\pi/2}^{\pi} \frac{1}{r_{\rm cor}}\mathrm{d}\phi + \int_{0}^{\pi/2} \frac{1}{r_{\rm cor}}\mathrm{d}\phi\right], \tag{38}$$

$$\Rightarrow \Delta t_1^{\rm AGBH} = \frac{I_1}{c} = \frac{8aM\{\chi[a(b+d_{OL}) + b(b+2d_{OL})] - b(a+b)\}}{b(a+b)c\chi d_{OL}}. \tag{39}$$

By taking the limit where the source and observer are both infinite distance away from the lens, that is when $d_{OL} \to \infty$, which also implies $d_{LS} \to \infty$, we have

$$\Delta t_1^{\rm AGBH} = \frac{8aM(a+2b)}{cb(a+b)}. \tag{40}$$

The requirement of thin-lens approximation further implies that $(a/b) \ll 1$ such that orders of $(a/b)^2$ and higher can be neglected, then we end up with

$$\Delta t_1^{\rm AGBH} \simeq \frac{16aM}{cb}, \tag{41}$$

which is independent of Q and is precisely the leading order delay obtained by Laguna & Wolszczan (1997) (also see footnote 2). Thus Equation (39) generalizes the zeroth-order TOA (41) to realistic finite distance thin-lens geometry.

In the same way, we can calculate the integrals I_2 and I_3 which, to leading orders in $(M/b)^2$ and $(M/b)^3$, work out to

$$\Delta t_2^{\rm AGBH} = \frac{I_2}{c} = \frac{4aM^2}{A_1 c(\chi d_{OL})^2}\{A_1\pi + A_2\chi d_{OL}(\chi - 1) + (A_1 + A_3 d_{OL}^2)\pi\chi^2\}\lambda_1, \tag{42}$$

$$\Delta t_3^{\rm AGBH} = \frac{I_3}{c} = \frac{2aM^3[4 - 4/\chi^3 + B_1 + B_2 + B_3]}{3cd_{OL}^3}\lambda_2, \tag{43}$$

Table 1. Some typical values of components Δt_1, Δt_2, and Δt_3 for the PSR-Cygnus X-1 binary. The last two columns contain the effect of the gyromagnetic ratio (Q/M). The distances d_{LS} and d_{OL} in Figure 1 are such that the angles remain small: $\gamma_1 \simeq \tan\gamma_1 = b/d_{LS} \simeq \delta_1 \simeq \tan\delta_1 \ll 1$, etc. The KBH values are given at $Q = 0$ (first row). Thus, even when the impact parameter b is 10,000 times farther than $r_{\rm ph}^{+}$, the first column of the table shows that the TOA component Δt_1 would be at the $\sim 0.03\,\mu$s level that could be measurable in near future. The other components in the table that contain (Q/M) are Δt_2 and Δt_3 but unfortunately they hold no promise to be measurable even in the far future apart from serving academic interest.

Q/M	χ	$\Delta t_1^{\rm AGBH,KNBH}$ (μs)	$\Delta t_2^{\rm AGBH,KNBH}$ (μs)	$\Delta t_3^{\rm AGBH}$ (μs)	$\Delta t_3^{\rm KNBH}$ (μs)
0 (KBH)	0.1	0.02825	1.1218×10^{-6}	4.8147×10^{-11}	4.8147×10^{-11}
0.5	0.1	0.02825	1.0517×10^{-6}	3.7615×10^{-11}	4.2129×10^{-11}
1	0.1	0.02825	0.8413×10^{-6}	0.6018×10^{-11}	2.4073×10^{-11}

Table 2. Some typical components Δt_1, Δt_2, and Δt_3 for SgrA* with values given by Kato (2010), viz., $M = 4.2 \times 10^6\, M_\odot$, $d_{OL} = 7.6$ kpc and a unique $a = 0.44\,M$ so that $r_{\rm ph}^{-} = 2.15 \times 10^{12}$ cm, $r_{\rm ph}^{+} = 1.51 \times 10^{12}$ cm, and $b = 10^7 r_{\rm ph}^{-}$ so that $M/b \ll 1$. The distances d_{LS} and d_{OL} in Figure 1 are such that the angles remain small: $\gamma_1 \simeq \tan\gamma_1 = b/d_{LS} \simeq \delta_1 \simeq \tan\delta_1$, etc. The KBH values are at $Q = 0$ (first row).

Q/M	χ	$\Delta t_1^{\rm AGBH,KNBH}$ (μs)	$\Delta t_2^{\rm AGBH,KNBH}$ (μs)	$\Delta t_3^{\rm AGBH}$ (μs)	$\Delta t_3^{\rm KNBH}$ (μs)
0 (KBH)	0.1	4.2117	1.9032×10^{-7}	9.2965×10^{-15}	9.2965×10^{-15}
0.5	0.1	4.2117	1.7842×10^{-7}	7.2629×10^{-15}	8.1345×10^{-15}
1	0.1	4.2117	1.4274×10^{-7}	1.1620×10^{-15}	4.6483×10^{-15}

where

$$A_1 = b^2(a+b)^2, \tag{44}$$

$$A_2 = 2b(a+b)(a+2b), \tag{45}$$

$$A_3 = a^2 + 2ab + 2b^2, \tag{46}$$

$$B_1 = \frac{4d_{OL}^3}{b^3} + \frac{4d_{OL}^3}{(a+b)^3}, \tag{47}$$

$$B_2 = \frac{3d_{OL}^2(\chi-1)}{\chi b^2} + \frac{3d_{OL}^2(\chi-1)}{\chi(a+b)^2}, \tag{48}$$

$$B_3 = \frac{3d_{OL}^2(\chi^2+1)}{\chi b^2} + \frac{3d_{OL}(\chi^2+1)}{\chi^2(a+b)}, \tag{49}$$

Equations (39) and (42)–(49) are the resulting TOA components to be used. For comparison purpose, we will compute the components for the well-known KNBH, which turn out to be

$$\Delta t_1^{\rm KNBH} = \frac{8aM\{\chi[a(b+d_{OL}) + b(b+2d_{OL})] - b(a+b)\}}{b(a+b)c\chi d_{OL}}, \tag{50}$$

$$\Delta t_2^{\rm KNBH} = \frac{4aM^2}{A_1 c(\chi d_{OL})^2}\{A_1\pi + A_2\chi d_{OL}(\chi-1) + (A_1 + A_3 d_{OL}^2)\pi\chi^2\}\xi_1, \tag{51}$$

$$\Delta t_3^{\rm KNBH} = \frac{2aM^3[4 - 4/\chi^3 + B_1 + B_2 + B_3]}{3cd_{OL}^3}\xi_2, \tag{52}$$

where

$$\xi_1 = 1 - \frac{Q^2}{4M^2}, \quad \xi_2 = 8 - \frac{4Q^2}{M^2}. \tag{53}$$

The same as in AGBH, the first-order effect, $\Delta t_1^{\rm AGBH} = \Delta t_1^{\rm KNBH}$, neither depends on (Q/M). Since $\lambda_1 = \xi_1$, it is evident also that $\Delta t_2^{\rm AGBH} = \Delta t_2^{\rm KNBH}$, so the difference in TOA between AGBH and KNBH will appear only in the third-order term Δt_3 onwards. For two astrophysical binaries, we shall plug the lens parameter values a and M, distance values b, d_{OL}, $\chi = d_{LS}/d_{OL}$ into the above equations, take care to preserve the smallness of the angles b/d_{OL}, $b/d_{LS} \ll 1$, and tabulate the components Δt_1, Δt_2, and Δt_3, the last two containing the factor Q/M (Tables 1 and 2).

5. Numerical estimates

Pulsar-BH (PSR-BH) binary systems provide the best laboratory for testing the difference in TOA predictions since variable sources such as pulsars, quasars, GRBs, etc., can give signals at the instant they are behind the spinning black hole on the optical axis *OL* and their TOA Δt can be measured at the observer *O*. Although a concrete example of such a binary is yet to be detected, the prospects for discovery seem quite promising (Laguna & Wolszczan 1997). We assume the pulsar orbit to be in the equatorial plane of the spinning lens and the line of sight is perpendicular to the axis of the spin.

5.1 *PSR-Cygnus X-1 binary*

An early estimate was that, of all pulsars discovered so far, a small but significant number of them belong to a PSR-BH category with a BH having masses a few times of solar masses (Lipunov *et al.* 2005). We consider a typical illustration, namely, of a PSR-Cygnus X-1 binary with $M = 14.8\,M_{\odot} = 2.19 \times 10^6$ cm, $a = 0.95\,M = 2.08 \times 10^6$ cm (Gou 2011), $d_{OL} = 1.86$ kpc $= 5.74 \times 10^{21}$ cm (Reid 2011). The KBH case corresponds to $Q = 0$, $\lambda_1 = 1$, and $\lambda_2 = 8$. The numerical value of $r^{\pm}_{\rm ph}$ for the spinning AGBH is practically insensitive to the small values of (Q/M) (Toshmatov 2014; Ahmed *et al.* 2019). The Kerr photon sphere radii should suffice, which are $r^{-}_{\rm ph} = 8.72 \times 10^6$ cm and $r^{+}_{\rm ph} = 3.05 \times 10^6$ ċm, so $r^{-}_{\rm ph}$ is the larger of the two radii. Accordingly, to preserve the thin-lens and PPN approximation, we choose, according to the stipulation in Section 4 (iii), $b = 10^4 r^{-}_{\rm ph} = 8.72 \times 10^{10}$ cm, so that $(M/b) \sim 10^{-5}$ justifying the PPN expansion in the curly bracket in Equations (26) and (27). Therefore, integrands rapidly converge. The lens–source distances $d_{LS} = \chi d_{OL}$ in Figure 1 are varied by varying χ but preserving the required smallness of the angles (in radian): $\gamma_1 \simeq b/d_{LS}$, $\delta_1 \simeq (a+b)/d_{LS}$, $\gamma_2 \simeq b/d_{OL}$, and $\delta_2 \simeq (a+b)/d_{OL}$.

5.2 *PSR-SgrA* binary*

Recent observations suggest that there are probably ~ 100 pulsars surrounding the supermassive spinning BH SgrA* with orbital periods $\lesssim 10$ years (Pfahl & Loeb 2004) and a few among them are expected to form PSR-BH binaries with stellar-sized BH companions residing within ~ 1 parsec of SgrA* (Faucher-Giguere & Loeb 2011). We shall assume the possibility that some of the pulsars cross the optical axis *OLS* behind SgrA* making a PSR-SgrA* binary.

We find that $\Delta t_1 \sim 4.2\,\mu$s allowed by the thin-lens approximation, which should be measurable with current technology provided an appropriate pulsar is identified in future missions.

6. Conclusion

Among the three categories of BHs, the AGBH is everywhere regular while the other two (KNBH and KBH) are centrally singular, all possessing significantly different qualitative behavior especially in the light cone structure and global properties. Such geometric differences stem from the fact that AGBH is sourced by nonlinear electrodynamics, whereas KNBH is sourced by a linear Maxwell field and KBH is a vacuum solution. One would naturally like to know if they differ from the observational point of view as well. To address the query, we chose a novel diagnostic, the difference in the TOA, which samples the frame-dragging effect of the spinning lens, and calculated the difference assuming the spinning lens partner in the binary to be the three BHs in succession. The generic formula for this purpose is Equation (25), which resulted in detailed Equations (39) and (42)–(53) under thin-lens approximation. The approximation implies that the TOA considered here is a weak field effect. They nevertheless allowed estimation of the effect of the gyromagnetic ratio (Q/M) on the TOA. The results are tabulated in Tables 1 and 2. To our knowledge, such a comparative study using the generic TOA Equation (25) has not been undertaken heretofore.

We wish to once again emphasize that the difference in the TOA is not the Shapiro gravitational time delay—they are fundamentally different physical effects. Enough attention has somehow not been paid to this important distinction, which is clearly explained in the introduction and specifically in footnote 2.

The method adopted in this paper can be applied with ease to any binary system assuming that the source, lens, and observer are aligned. An added advantage offered by Equations (39) and (42)–(53) is that they take into account the finite distance thin-lens geometry, which truly describes the realistic astrophysical lens configuration. The resulting order of magnitude estimates for Δt_1, Δt_2, and Δt_3 from Equations (39) and (42)–(53) are tabulated for the

three illustrative binary systems. They are quite robust, that is, the order of magnitudes remains unaltered even when the observer–lens distance indicator χ and the gyromagnetic ratio (Q/M) are varied at will preserving small angles respecting the thin-lens approximation. However, these estimates are to be taken as only suggestive, since no binary system has yet been conclusively identified, although Monte Carlo simulations indicate that the number of PSR-BH binaries could be significant with a spinning BH companion having a few solar masses (Gou 2011). We have considered two binary systems, PSR-Cygnus-X1 and PSR-SgrA*, and the zeroth-order delays have been found to be at the μs level quite consistent with similar predictions in the literature (Laguna & Wolszczan 1997).

The prediction of Δt_1 based on Equation (39) for the PSR-Cygnus-X1 system is about 0.028 μs (Table 1). Achieving the required level of accuracy could be possible in the near future since a precision of 0.1 μs was achieved by Van Straten (2001) for PSRJ0437-4715, a bright millisecond pulsar in a White Dwarf-Neutron Star binary system. However, the measurement of higher-order terms Δt_2 and Δt_3 that contain (Q/M) would require better than pico-second level accuracy, which is unlikely to be attained even in the far future. As to the PSR-SgrA* binary, it is found that $\Delta t_1 \sim 4.11$ μs (Table 2), which should be measurable provided a suitable variable source is detected from among the pulsars orbiting SgrA* (Kato 2010; Faucher-Giguere & Loeb 2011) and other complications are taken care of.

Since the effect of (Q/M) on the difference in TOA is rather tiny in the ideal situation considered above, it may be that TOA is not the best diagnostic. Alternatively, we might think that the predictions might be improved by considering the arrival times at O along the exact null trajectories grazing the BH photon spheres $r_{\rm ph}^{\pm}$ like one does in the case of computing lensing observables in the strong field limit (Nandi *et al.* 2017, 2018; Izmailov *et al.* 2019b,c). In this case, of course, the weak field thin-lens approximation will break down although it provides a "simple and elegant description of many realistic lensing situations" (Hartle 2003). The strong field limit has its share of woes, one of which is the following: To calculate exact null path lengths, one needs to know the exact bending, but unfortunately the latter reveals a virulent logarithmic divergence at the photon sphere preventing a Taylor expansion around it. One way to tackle this problem could be to consider a different expansion, the so-called "affine perturbation series," that has been claimed to work up to 1% accuracy to the exact value (Iyer & Petters 2007; Iyer & Hansen 2009). We shall deal with these issues in future work.

For completeness, we comment on some subtleties associated with light propagation in a nonlinear electromagnetic field. We emphasize that in our work we adhered strictly to Einstein's theory of gravity. Thus, the nonlinear electrodynamics form the stress tensor on the right-hand side of Einstein's field equations resulting in the exact solution of AGBH, which subsumes the electromagnetic nonlinearity in its curved geometry. Light follows null geodesics of that curved space–time, $\mathrm{d}\tau^2 = 0$, which is what we had considered in accordance with Einstein's theory. The flat background cannot be separated from the curved geometry due to the universality of gravitation. On the other hand, the work by Novello (2000) suggests a space–time completely different from that of AGBH. The light propagation in a nonlinear electrodynamic field placed on top of a flat Minkowski background with metric $\eta^{\mu\nu}$ does not follow geodesics of $\eta^{\mu\nu}$ but can be thought of as following the geodesics of an "effective" curved space–time $g_{\rm eff}^{\mu\nu}$ that has nothing to do with the AGBH space–time. It was already recognized in the work of Novello *et al.* (2000) that the analogy between photon propagation in effective space–time and its behavior in a true gravitational field cannot be pushed too far except merely that in both cases there occur curved geometries resulting from the corresponding nonlinear processes. There is two entirely different space–times arising here—one is the exact AGBH from Einstein's theory and the other is the effective space–time perceived by photons alone. Studying TOA in effective geometry would certainly be interesting future work.

Note further that the effective metric $g_{\rm eff}^{\mu\nu}$ for Born–Infeld electrodynamics is based on the flat Minkowski background metric $\eta^{\mu\nu}$ in Euclidean coordinates is given by Plebansky (1968) and Novello (2000)

$$g_{\rm eff}^{\mu\nu} = \left(b^2 + \frac{1}{2}F\right)\eta^{\mu\nu} + F^{\mu}_{\lambda}F^{\lambda\nu},$$

where b^2 is related to the Born–Infeld electric field parameter. In virtue of the principle of general covariance, one could convert $\eta^{\mu\nu} \to \gamma^{\mu\nu}$ in non-Euclidean coordinates but that would not introduce any new physics. However, if the effective metric $g_{\rm eff}^{\mu\nu}$ is based not on a flat background $\gamma^{\mu\nu}$ but on a background metric $g^{\mu\nu}$ for which the curvatures are non-vanishing, then $g_{\rm eff}^{\mu\nu}$ would describe photon propagation in nonlinear electrodynamics placed on

top of an already curved background $g^{\mu\nu}$. The work by Jana & Kar (2015) provides an exemplary exercise in this generalized framework applied to the Born–Infeld electrodynamics.

When this article was under review, very recent work by Toshmatov *et al.* (2021) came to our notice. Using the notion of effective metric, they show that for any black hole being a charged solution of the field equations of GR coupled to the nonlinear electrodynamics, one cannot distinguish the two types of charges (magnetic and electric) through the motion of light rays around it. This is certainly a new and important conclusion that could have far-reaching consequences. However, in the present paper, the considered AGBH metric is not an effective metric perceived by the motion of light alone but is an exact solution—its geodesics describe the motion of both light and particles alike respecting the universality of gravitation.

Acknowledgements

The authors thank an anonymous reviewer for his/her constructive comments.

References

Abdujabbarov A. *et al.* 2016, Phys. Rev. D, 93, 104004
Ahmed F., Amir M., Ghosh S. 2019, Astrophys. Space Sci., 364, 10
Ayón-Beato E., García A. 1998, Phys. Rev. Lett., 80, 5056
Bhadra A., Nandi K. K. 2010, Gen. Rel. Grav., 42, 293
Born M., Infeld L. 1934a, Proc. R. Soc. Lond., A, 143, 410
Born M., Infeld L. 1934b, Proc. R. Soc. Lond., A, 144, 425
Boyer R. H., Lindquist R. W. 1967, J. Math. Phys., 8, 265
Bronnikov K. A. 2000, Phys. Rev. Lett., 85, 4641
Datta B., Kapoor R. C. 1985, Nature, 315, 557
Deng X. -M., Xie Y. 2017, Phys. Lett. B, 772, 152
Dymnikova I. G. 1984, Sov. Phys.—JETP, 59, 223
Dymnikova I. G. 1986, Sov. Phys.—Usp., 29, 215
Faucher-Giguere C. A., Loeb A. 2011, Mon. Not. R. Astron. Soc., 415, 3951
Ghosh S., Bhadra A. 2015, Eur. Phys. J. C, 75, 494
Ghosh S., Bhadra A., Mukhopadhyay A. 2019, Gen. Rel. Grav., 51, 54
Gou L. *et al.* 2011, Astrophys. J., 742, 85
Hartle J. B. 2003, Gravity: An introduction to Elnstein's general relativity. Pearson Inc., p. 237
Iyer S. V., Petters A. O. 2007, Gen. Rel. Grav., 39, 1563
Iyer S. V., Hansen E. C. 2009, Phys. Rev. D, 80, 124023
Izmailov R. N. *et al.* 2019a, Eur. Phys. J. C, 79, 105
Izmailov R. N. *et al.* 2019b, Mon. Not. R. Astron. Soc., 483, 3754
Izmailov R. N. *et al.* 2019c, Eur. Phys. J. Plus, 134, 384
Izmailov R. N. *et al.* 2020, Ann. Phys. 413, 168069
Jana S., Kar S. 2015, Phys. Rev. D, 92, 084004
Karimov R. Kh. *et al.* 2018a, Eur. Phys. J. Plus, 133, 44
Karimov R. Kh. *et al.* 2018b, Gen. Rel. Grav., 50, 44
Kato Y. *et al.* 2010, Mon. Not. R. Astron. Soc., 403, L74
Kulbakova A. *et al.* 2018, Class. Quantum Grav., 35, 115014
Laguna P., Wolszczan A. 1997, Astrophys. J., 486, L27
Lipunov V. M., Bogomazov A. I., Abubekerov M. K. 2005, Mon. Not. R. Astron. Soc., 359, 1517
Manko V. S., Ruiz E. 2016, Phys. Lett. B, 760, 759
Matilsky T., Shräder C., Tananbaum H. 1982, Astrophys. J., 258, L1
Nandi K. K. *et al.* 2017, Phys. Rev. D, 95, 104011
Nandi K. K. *et al.* 2018, J. Cosmol. Astropart. Phys., 07, 027
Nandi K. K. *et al.* 2020, Phys. Lett. B, 809, 135734
Newman E. T., Janis A. I. 1965, J. Math. Phys., 6, 915
Novello M. *et al.* 2000, Phys. Rev. D, 61, 045001
Pfahl E., Loeb A. 2004, Astrophys. J., 615, 253
Plebansky J. 1968, *Lectures on Nonlinear Electrodynamics* (Nordita, Copenhagen)
Reid M. J. *et al.* 2011, Astrophys. J., 742, 83
Shapiro I. I. 1964, Phys. Rev. Lett., 13, 789
Toshmatov B., Ahmedov B., Malafarina D. 2021, Phys. Rev. D, 103, 024026
Toshmatov B. *et al.* 2014, Phys. Rev. D, 89, 104017
Toshmatov B. *et al.* 2015, Phys. Rev. D, 91, 083008
Tuleganova G. Y. *et al.* 2020, Gen. Rel. Grav., 52, 31
Tuleganova G. Y., Muhamadieva L.Y. 2021, Astrophys. Space Sci., 366, 8
Van Straten W. *et al.* 2001, Nature, 412, 158